METALURGI
Majalah Ilmu dan Teknologi
p-ISSN 0126-3188 | e-ISSN 2443-3926
ejurnalmaterialmetalurgi.lipi.go.id

PRELIMINARY STUDY OF MATERIAL PROPERTIES ON PU-Mg AND PU-Zn FOR ANEURYSM CLIP APPLICATION

Made Subekti Dwijaya*, Talitha Asmaria
Research Center for Metallurgy, National Research and Innovation Agency
Management Building 720, B.J. Habibie Sains and Technology Area, Banten, Indonesia 15343
*E-mail: made004@brin.go.id

Received: 13-05-2022, Revised: 19-07-2022, Accepted: 04-10-2022

Abstract

An aneurysm clip is an implant tool for assisting the neurosurgeon in treating acute hemorrhagic stroke and cerebral aneurysm. This equipment stops the blood flow of a ruptured or enlarged blood vessel or aneurysm. In the development of aneurysm clip production, titanium alloy is the most used material selection. Several researchers reported that this metal leads to artifacts during MR (magnetic resonance) or CT (computed tomography) imaging. Since several pieces of evidence polyurethane could be a good material selection for aneurysm clips, this paper aims to investigate the material properties of the polyurethane foam with an additional combination of magnesium and zinc. This study conducts magnesium and zinc composition variations of 1 wt.%, 2 wt.%, and 3 wt.%, respectively. The materials were tested using a compression test, a FTIR (fourier-transform-infrared), SEM (scanning-electron-microscope), DSC (differential-scanning-calorimetry), and TGA (thermogravimetric-analyzer) to determine the material properties. From all examinations, adding magnesium and zinc to polyurethane foam affected the compressive strength and porosity of the polyurethane foam. Therefore, all test results concluded that adding magnesium with a composition of 3wt.%, which has a compressive strength of 0.84 MPa, is the best mixture. The idea of finding other compositions that are compatible with the polyurethane will significantly increase the possibility of new materials for aneurysm clip construction.

Keywords: *Aneurysm clip, compressive strength, magnesium, polyurethane foam, zinc*

1. INTRODUCTION

Aneurysm clip is one of the neurosurgery management tools to treat by clamping the blood vessels [1]-[2]. Several health conditions, such as acute hemorrhagic stroke and cerebral aneurysm, require a specific operation to close the aneurysm or the area of the blood vessel that is ruptured or enlarged by using a clip with metal material in the blood vessel. A hemorrhagic stroke happens because of a blood vessel rupture that acts as a blood supply to the brain. In cases of acute hemorrhagic stroke, surgery is one of the recommended actions because it is an effort to stop bleeding, reduce pressure in the skull, increase the possibility of recovery and reduce the death rate from stroke [1]. Furthermore, cerebral aneurysms are a kind of cerebrovascular illness in which a weakening of a cerebral artery results in an abnormal focal dilation. The therapies of microsurgical and endovascular have two aims; to remove brain aneurysms from the cerebral circulation and to prevent them from rupturing [3]. Another treatment for cerebral aneurysms is surgical clipping, ensuring the cerebral aneurysm from blood flowing with a clip.

An ideal aneurysm clip model requires these features: small size, biocompatibility, low cost, good mechanical properties (such as tensile strength, corrosion resistance, and fatigue resistance), and common image artifacts [4]. The innovation of aneurysm clip was started by Helbert Olivercona (1891-1980), followed by many contributors; those were Frank Mayfield (1908-1991), Charles Drake (1920-1998), Joseph McFadden (1920-present), Thoralf Sundt Jr. (1930-1992), William M. Lougheed (1923-2004), William B. Scoville (1906-1984), Milton D. Heifetz (1921-2015), Gazi Yasargil (1925-present), Kenichiro Sugita (1932-1994), and Robert Spetzler (1944-present)[5]. Based on this

DOI : 10.14203/metalurgi.v37i2.645

Metalurgi is Sinta 2 Journal (https://sinta.ristekbrin.go.id/journals/detail?id=3708) accredited by Ministry of Research & Technology, Republic Indonesia

last review paper about the origins of eponymous aneurysm clips, the innovation in medicine, including aneurysm clips, is significant in supporting aneurysm surgery. Designs and material selection are the most consideration in the manufacturing technology of aneurysm clips. In developing aneurysm clip materials, Ti6Al4V is the most used material. Like most metal implant materials, Ti6Al4V has good mechanical properties and biocompatibility, low density, good corrosion resistance, and low young's modulus of 55-110 GPa. Although Ti6Al4V has a higher Young's modulus than the bone, around 10-30 GPa, it has a significantly lower Young's modulus compared to other biocompatible metals, which are CoCr around 240 GPa and SS316L around 240 GPa[6]-[8].

Besides that, the titanium alloy could cause artifacts in MRI (magnetic resonance imaging), which could aggravate the aneurysm and the surrounding tissue diagnosis [9]. Kocasarac et al.'s research show that the titanium and titanium alloy implants produced high susceptibility artifacts on MRI that caused decreasing quality images due to large signal voids[10]. Ito et al. examined the artifacts caused by titanium clips on MR (magnetic resonance) images and detected the artifact sizes 200% larger than the size of the actual clips [11]. Another study by Khursheed et al. revealed that the largest artifact produced by titanium alloy aneurysm clip takes up 3.94% of brain volume, and the artifact/clip length ratio is 4.75 to 6.55 mm [12]. Based on the evidence presented, another material is considered for an aneurysm clip, and one of them is a polymer.

Magnesium as an implant material is widely used in many surgical applications. Its lightweight, biocompatible and has sufficiently good mechanical properties. Moreover, the MRI artifact generated by magnesium is less severe than the titanium implant, demonstrating a superior 3D image reconstruction quality compared to titanium [13]. In medical imaging, a magnesium implant has beneficial properties compared to other metal implants. Conventional radiography showed only small attenuation using the magnesium and was lower than the Titanium imaging. Moreover, in MRI, magnesium produced fewer artifacts than titanium, which could ease the imaging evaluation in postoperative [14].

A solid fiducial marker is usually made of high atomic materials such as gold. However, such materials generate streak artifacts which affect the radiation dose calculation and post-treatment assessment. A suitable fiducial marker should minimize artifacts. Zinc has a 7.14 g/cm^3 density, which is 37% of gold. The atomic number of zinc is 30, much lower than gold but five times of carbon. Zinc is also known for its biocompatibility and low toxicity degradation release (0.15mg/day, the toxicity threshold is 100-150mg/day) [15].

Polymer is one of the biomedical implant materials thanks to its biocompatibility, biostability, and noncytotoxic. Gas and water permeability are also calculated to protect the electronic circuit device from moisture and ions within the body [16]. Due to its wide range of options and achieved requirements, polymer-based for aneurysm clips are developed these days. W. S. Cho et al., showed that polyurethane and PDMS (polydimethylsiloxane) was the perfect candidates for aneurysms clip material [17]. Polyurethane has a higher value than PDMS, considering the elastic modulus and strain to failure. Polyurethanes are synthetic polymers that feature hard and soft microstructures. Diisocyanates with low molecular weight and high glass transitions form the hard phase. Thus, this study chose polyurethane for the aneurysm clip materials.

On the other hand, the soft phase comprises polyols with low glass transitions. This polymeric material has 90.1± 0.3°Sh A hardness with 7.2 ± 0.2 MPa. The polyurethane chains can be incorporated into active substances to improve the mechanical properties and meet the requirements of an aneurysm clip [18]. In 2018, Won-Sang Cho et al. researched an aneurysm clip made of zirconia-polyurethane with MR compatibility and mechanical properties to minimize the imaging artifacts [17]. They used commercial 3 mol% Y_2O_3-stabilized ZrO_2 and TiO_2 for the clip body and polyurethane and PDMS for the head spring. The MR susceptibility test showed minor artifacts; the artifact volume is 2.6 times larger than the real one. Polyurethane showed a higher elastic modulus than PDMS, so polyurethane was chosen to be the head spring. There are not many polymer-based aneurysm clips developed.

This paper aims to fabricate polymer-based aneurysm clips to minimize the CT (computed tomography) imaging artifacts by adding 1, 2, and 3 wt.% magnesium powder and 1, 2, and 3 wt.% zinc powder. The material will be tested with FTIR (fourier-transform-infrared), SEM (scanning-electron-microscope), DSC (differential-scanning-calorimetry), TGA (thermogravimetric-analyzer) and a compression test. This paper will significantly contribute to

developing material selection for the aneurysm clips.

2. MATERIALS AND METHODS

Polyurethane parts A (isocyanate part) and B (polyols part) with a volume ratio of 2:1 were prepared. First, the isocyanate part, the polyols part of PU (polyurethane), and the 1, 2, & 3 wt.% of magnesium and zinc powder were added into the mold. The blend stirred for 3 minutes at a constant rate; after the free rise foam process was completed, the foam synthesis continued by a curing process at ambient temperature for 24 hours. After 24 hours, the PU foam was cut into three cubes with dimensions 5 x 5 x 5 cm according to ASTM D1621-16. PU pure was used as the reference foam. Table 1 shows the foam grouping .

All foams were characterized using FTIR (fourier transform infrared) to confirm the urethane compound, indicating successful polymerization. SEM (scanning electron microscope) was used to examine the morphology of the foam surface. The glass transition temperature (Tg) was analyzed using DSC (digital scanning calorimetry). TGA (thermogravimetric analyzer) to determine the thermal stability of the foam and compression test to determine the compressive strength of the foam.

Table 1. PU, PU-Mg, & PU-Zn foam grouping

Materials	1 wt. % Mg	2 wt. % Mg	3 wt. % Mg	1 wt. % Zn	2 wt. % Zn	3 wt. % Zn
PU Pure	-	-	-	-	-	-
PU-Mg1	√	-	-	-	-	-
PU-Mg2	-	√	-	-	-	-
PU-Mg3	-	-	√	-	-	-
PU-Zn1	-	-	-	√	-	-
PU-Zn2	-	-	-	-	√	-
PU-Zn3	-	-	-	-	-	√

3. RESULT AND DISCUSSION

3.1 FTIR (Fourier Transform Infrared) Analysis Result

The FTIR (fourier transform infrared) characterization aims to determine chemical compounds based on atomic bonds. Through this characterization, the functional groups formed in the composite material can also be seen.

Polyurethane is a polymer formed from the reaction between a polyol's OH (hydroxyl) group and with NCO (isocyanate functional group). In pure polyurethane (without adding other elements), the results of the FTIR test can be seen in Figure 1. There are two general methods to fabricate polyurethane foam, and both involve excessive diisocyanate on termination. The first method is pre-polymer termination using diisocyanate, and the second is polyol termination using diisocyanate, followed by adding a crosslinker [19]. The peak list is presented in Table .

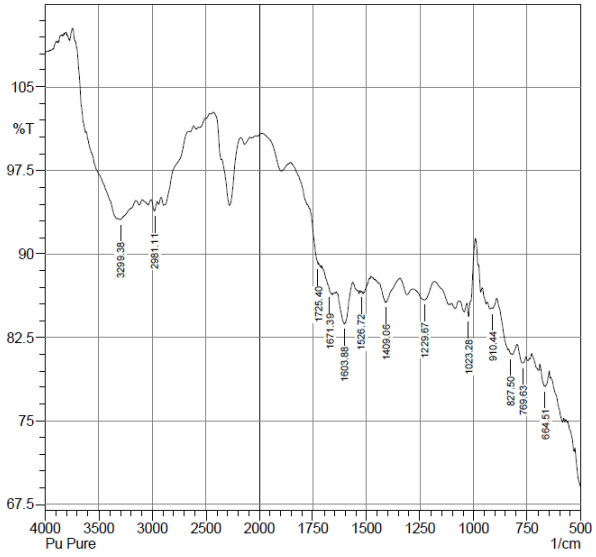

Figure 1. FTIR graph for pure polyurethane

There are three types of H-bonds in polyurethane, namely: an NH group that binds an H to one of three possible groups of proton acceptors; (a) carbonyl groups, (b) C-O-C polyethers, and (c) oxygen alkoxy urethanes [20]. In pure polyurethane foam, a stretching NH bond at 3299.38 cm^{-1} indicates the urethane compound.

Table 2. Peaks for pure polyurethane

Peak (cm^{-1})	Compound
910.44	C-O-C stretching
1023.28	Cyanate (-OCN dan C-OCN stretch)
1526.72	C-N stretching
1603.88	
1671.39	C=O stretching
1725.40	
2981.11	CH stretching
3299.38	NH stretching

3.1.1 FTIR of Polyurethane with Addition of Mg

The FTIR characterization was performed to determine the chemical compounds in the polyurethane mixture by adding magnesium (Mg) with a ratio of 1, 2, and 3 wt.% of Mg. The results of the FTIR characterization are shown in Figure 2.

Polyurethane itself is a polymer formed from the reaction between OH (hydroxyl) groups of polyols, which were shown at peaks of 3320.2038 cm^{-1} to 3323.0635 cm^{-1} (PU-Mg1-3), with NCO (groups of PU-Mg1-3). Isocyanate

function, shown at the peak of ~2269.2349 cm^{-1} in all PU-Mg foam. In all PU-Mg foam, NH stretching bonds showed at about 3017.0672 cm-1 to 3031.3661 cm^{-1}. C-O-C stretching bonds are shown at the peak of 1292.6202 cm^{-1} and 1294.0501 cm^{-1} for the three PU-Mg foam. In contrast, 1611.4856 cm^{-1} for PU-Mg1 and 1612.9155 cm^{-1} peaks for PU-Mg2 and PU-Mg3 showed the C=O stretching bond.

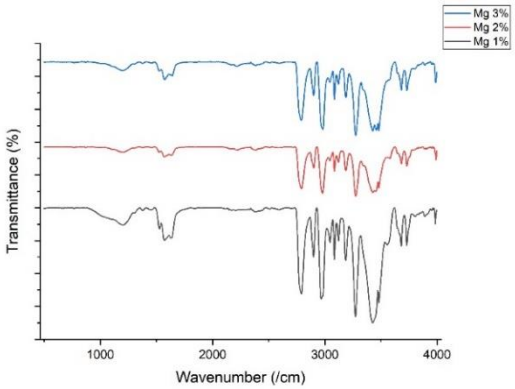

Figure 2. FTIR graph of polyurethane with addition of Mg

The FTIR spectral variations on C-O-C stretching, NH stretching, and C=O stretching can be used well as an indicator of the presence of H-bonds between oxygen alkoxy urethane and NH groups. Based on the results of the FTIR test in Table 3, the PU-Mg foam reveals several peaks with each type of bond.

Table 3. Peaks for polyurethane with Mg

Specimen	Peak (cm^{-1})	Compound
PU-Mg 1 wt.%	1112.4541	Cyanate (-OCN and C-OCN stretch)
	1294.0501	C-O-C stretching
	1611.4856	C=O stretching
	2269.2349	Isocyanate (-N=C=O stretch)
	3017.0672	NH stretching
	3320.2038	OH stretching
PU-Mg 2 wt.%	1111.0242	Cyanate (-OCN and C-OCN stretch)
	1292.6202	C-O-C stretching
	1612.9155	C=O stretching
	2296.4028	Isocyanate (-N=C=O stretch)
	3031.3661	NH strectching
	3323.0635	OH stretching
PU-Mg 3 wt.%	1292.6202	C-O-C stretching
	1612.9155	C=O stretching
	2269.4028	Isocyanate (-N=C=O stretch)
	3025.6465	NH strectching
	3323.0635	OH stretching

3.1.2 FTIR of Polyurethane with Addition of Zn

The FTIR test was carried out to determine the chemical compounds in the polyurethane mixture by adding zinc (Zn) with a ratio of 1, 2, and 3 wt.% Zn. The comparison of the FTIR test results to the specimens is shown in Figure 3.

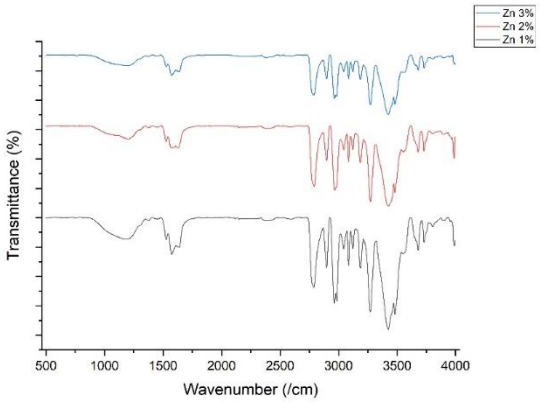

Figure 3. FTIR graph of polyurethane with addition of Zn

Table 4 shows the peak lists of polyurethane with the addition of Zn. PU-Zn foam shows several peaks with each type of bond. Polyurethane formed from the reaction between OH (hydroxyl) groups of polyols, shown at peaks of 3318.7739 cm^{-1} to 3321.6336 cm^{-1} (PU-Zn1-3), with NCO (groups PU-Zn1-3). The isocyanate function group was confirmed at 2269.2349 cm^{-1} in all three foams. The FTIR result also confirmed the presence of Zn in PU at peaks of 1542.8509 cm^{-1} for PU-Zn1, 1541,4210 cm-1 for PU-Zn2, and 1542.8509 cm^{-1} for PU-Zn3. It overlaps with the amide zone II.

In the three foams, NH stretching bonds at about 3015.6373 cm^{-1} and 3017.0672 cm^{-1}. C-O-C stretching bonds were shown at 1193.9578 cm^{-1} and 1295.48 cm^{-1} for PU-Zn2 and PU-Zn3. In comparison, ~1612.9155 cm^{-1} peak showed the C=O stretching bond for the three foams.

Table 4. Peaks for polyurethane with Zn

Specimen	Peak (cm^{-1})	Compound
PU-Zn 1 wt.%	1181.0885	Cyanate (-OCN dan C-OCN stretch)
	1612.9155	C=O stretching
	2269.2349	Isocyanate (-N=C=O stretch)
	3017.0672	NH stretching
	3321.6336	OH stretching
PU-Zn 2 wt.%	1112.4541	Cyanate (-OCN dan C-OCN stretch)
	1295.48	C-O-C stretching
	1611.4856	C=O stretching
	2269.2349	Isocyanate (-N=C=O stretch)
	3015.6373	NH strectching
	3318.7739	OH stretching
PU-Zn 3 wt.%	1112.4541	Cyanate (-OCN dan C-OCN stretch)
	1193.9578	C-O-C stretching
	1612.9155	C=O stretching
	2269.2349	Isocyanate (-N=C=O stretch)
	3015.6373	NH strectching
	3320.2038	OH stretching

3.2 Compression Test Analysis

The compression test used for rigid polymeric foam was in accordance with ASTM D1621-16. The test specimen is prepared in a cube shape or tube with a minimum area of 25,8 cm2 (4 in^2) and a maximum area of 232 cm^2 (36 in^2). The maximum height can't be more than the width or diameter of the specimen. The compression test determined the compressive strength of polyurethane with 1, 2, and 3 wt.% magnesium powder. The compression test result of the PU-Mg & PU-Zn group is shown in Figs 4 and 5.

For the PU-Mg group, the PU-Mg3 gave the highest compression strength at 0.84 MPa, while the PU-Zn3 gave the highest compression strength at 0.392 MPa, as shown in Fig. 5. The compression test results of PU-Mg and PU-Zn show a similar trend. The compressive strength increased along with the increasing amount of magnesium or zinc powder.

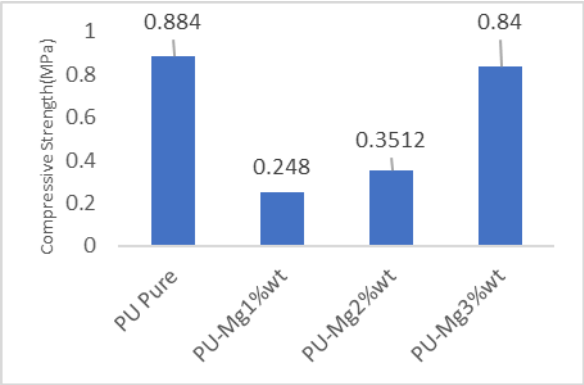

Figure 4. Compressive strength of PU-Mg

However, the PU Pure achieved the highest compression strength of all foams at 0.884 MPa. The lower compression strength of PU-Mg and PU-Zn compared to the PU pure was attributed to the weak interface between the additive and the matrix. The higher amount of incorporation of Mg and Zn powder into the PU matrix causes the additive to agglomerate due to the poor dispersion of the additive particle [21].

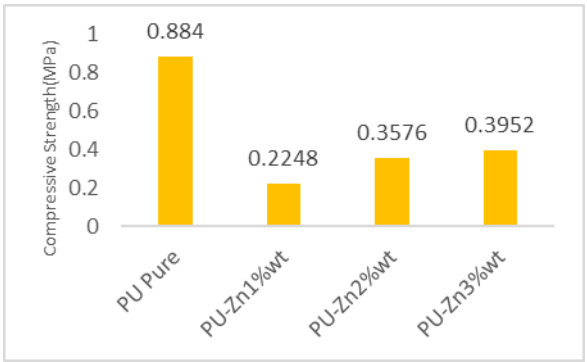

Figure 5. Compressive strength of PU-Zn

In general, inorganic fillers cause the foam cell to be more open, which lowers the mechanical properties. Moreover, the low compatibility between the inorganic fillers and the PU tends to cause cracking at the interfaces [22]

3.3 SEM (Scanning Electron Microscope) Analysis

SEM (scanning electron microscope) is used to observe the morphology of the foam surface.

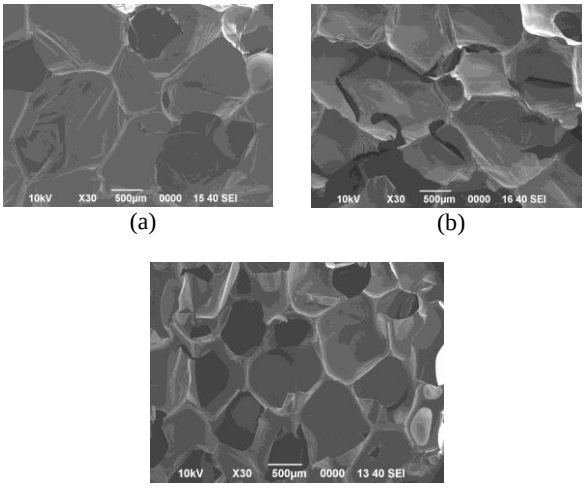

(a) (b)

(c)

Figure 6. SEM Results for polyurethane with Mg addition (wt.%); (a) 1, (b) 2, and (c) 3

The SEM results for polyurethane with the addition of magnesium (Mg) with a ratio of 1, 2, and 3wt.% Mg are shown in Fig. 6. SEM results of PU-Mg show a porous structure. Table 5 shows the more amount of magnesium added, the smaller the cell size of the foam.

Table 5. Polyurethane/Mg porosity

Mg Composition (wt.%)	Porosity (%)	Porosity length (µm)
1	88.816	1078.793
2	81.550	1050.352
3	81.209	1012.350

Changes in cell morphology characterized by changes in the size of small and large cells may be related to the presence of Mg, which affects the foaming process of PU/Mg [21].

Adding Mg of 3 wt.% will show a more distorted cell shape, damaged cell walls, and less homogeneous cell structures. The polyurethane morphology with the addition of 1, 2, and 3 wt.% zinc was shown in Fig. 7. Table 6 shows that the results of the SEM test of PU-Zn foam have a porous structure.

Polyurethane foam has a cellular structure and consists of partially open cells with circular holes. This result also shows that the greater the zinc

composition added, the smaller the porosity of the specimen. Zn particles act as the initial site of nucleation (cell formation).

Table 6. Polyurethane/Zn porosity

Zn composition (wt.%)	Porosity (%)	Porosity length (µm)
1	77.749	941.3328
2	77.571	881.9152
3	77.256	768.6748

However, at the same time, the addition of Zn will inhibit cell growth and produce smaller cell sizes [23].

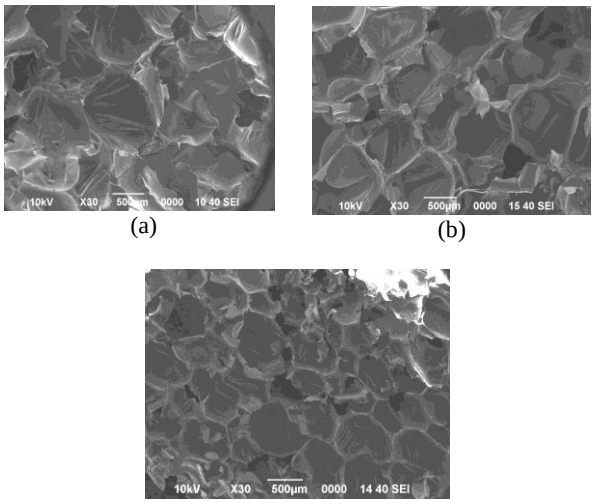

(a) (b) (c)

Figure 7. SEM results for polyurethane with Zn addition (wt.%); (a) 1, (b) 2, and (c) 3

3.4 DSC (Differential Scanning calorimetry) Analysis

The DSC (differential scanning calorimetry) characterization was performed from 40 °C to 350 °C with a heating rate of 5 °C/min. The results of the DSC test are in the form of a thermogram that can provide information about the thermal properties of a polymer, which is Tg in each foam. The foam used for testing has a minimum weight of 3 mg.

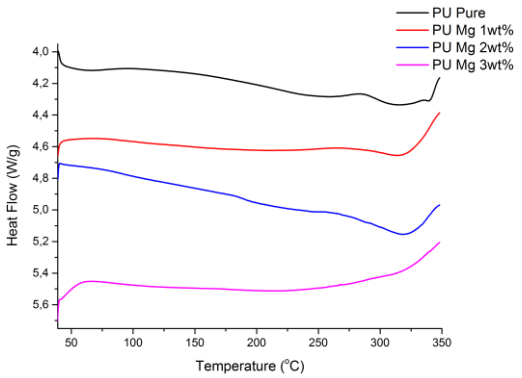

Figure 8. DSC result of PU Pure and PU-Mg series

Variations in the addition of the amount of magnesium and the amount of zinc were used to identify the trend of each of these variations. The results of the DSC are shown in Figs. 8 and 9.

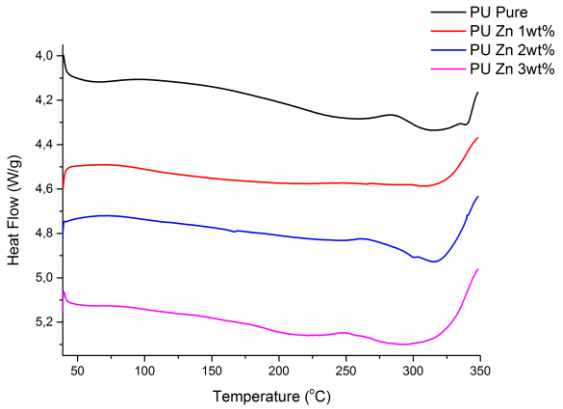

Figure 9. DSC result of PU Pure and PU-Zn series

Table 7 shows that the more Mg or Zn is added, the higher the glass transition temperature (Tg). The increases in the concentration of the additives reduce the molecular mobility of the matrix, which results in the shift of the foams Tg to a higher temperature [24]. The DSC result also supports the SEM test results shown in Fig. 6 and Fig. 7 because the pore size gets smaller with the addition of Mg or Zn, so the mobility of the molecule is limited.

Table 7. Glass transition temperature (Tg) for each foams

Materials	Tg (°C)
PU Pure	112.8
Mg 1 wt.%	124.16
Mg 2 wt.%	189.66
Mg 3 wt.%	185.92
Zn 1 wt.%	120.13
Zn 2 wt.%	122.60
Zn 3 wt.%	159.40

3.5 TGA (Thermogravimetric Analysis) Result

The TGA (thermogravimetric analysis) was performed by heating the foam from 40 to 450 °C at a heating rate of 5 °C/min.

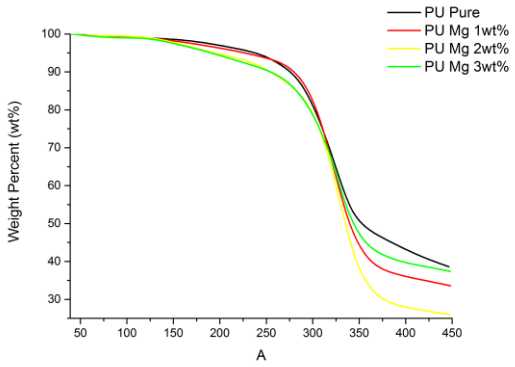

Figure 10. TGA result of polyurethane with Mg

The TGA results show how much the material decomposes as it's heated [25].

Figure 10 and Figure 11 show the result of TGA. The decomposition temperature for all foams is shown in Table 8. The initial decomposition temperature shows a 5 wt.% decrease in the foam weight due to the evaporation of water vapor contained in the foam.

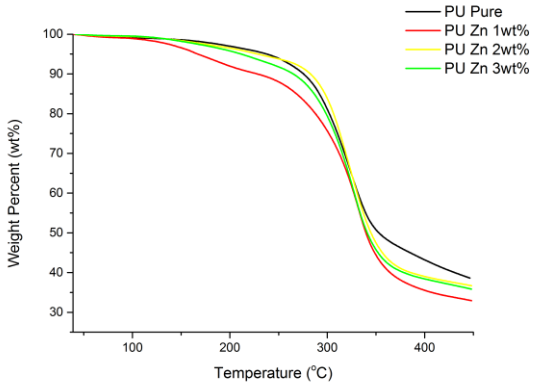

Figure 11. TGA result of polyurethane with Zn

PU Pure foam shows the highest temperature at 237.97 °C, while PU-Mg1 shows the lowest temperature at 166.96 °C. The decomposition peak temperature shows the degradation temperature of polyurethane's soft segment, which consists of the polyol part. The PU-Mg & PU-Zn series foam has a higher temperature than the PU pure, indicating that the incorporation of additives could increase the PU foam's thermal stability [19].

Table 8. Decomposition temperature for each foam

Composition	Initial Decomposition Temperature (°C)	Decomposition peak temperature (°C)	Weight Loss (%)
PU Pure	237.97	350.30	61.384
Mg 1 wt.%	227.05	363.79	54.940
Mg 2 wt.%	195.15	373.94	57.073
Mg 3 wt.%	190.37	380.19	47.856
Zn 1 wt.%	166.96	356.38	50.946
Zn 2 wt.%	228.86	369.41	52.168
Zn 3 wt.%	211.46	374.36	50.488

4. CONCLUSION

The effect of adding of magnesium or zinc to the polyurethane foam, which would serve as a potential aneurism clip material, was detailed. Several tests were conducted to know the mechanical and thermal properties. All foams show the bond between hydroxyl and isocyanate function on FTIR (fourier transform infrared) testing resulting from polyurethane foam formation. Adding 1, 2, and 3 wt.% of magnesium will increase the compressive strength, glass transition temperature (Tg), initial decomposition temperature, decomposition peak temperature, and weight loss, also decreasing the porosity area and length. As well as the addition of 1, 2, and 3 wt.% zinc will also increase the compressive strength and glass transition temperature (Tg), decreasing the porosity area and length, initial decomposition temperature, decomposition peak temperature, and weight loss. The polyurethane foam, with the addition of 3 wt.% magnesium (PU-Mg3), achieves the best result with a compressive strength of 0.84 MPa.

ACKNOWLEDGMENT

The author thanks to Erika Satriana and Farah Zafira Rennu for the helps in several experiments on this study.

REFERENCES

[1] D. F. Louw, W. T. Asfora, and G. R. Sutherland, "A brief history of aneurysm clips.," *Neurosurg. Focus*, vol. 11, no. 2, 2001. Doi: 10.3171/foc.2001.11.2.5.

[2] J. P. Mohr, P. A. Wolf, J. A. Grotta, M. A. Moskowitz, M. Mayberg, and R. von Kummer, *Stroke: Pathophysiology, Diagnosis, and Management*. Elsevier, pp. 589-613, 2011.

[3] S. Marbacher, F. Strange, J. Frösén, and J. Fandino, "Preclinical extracranial aneurysm models for the study and treatment of brain aneurysms: A systematic review," *J. Cereb. Blood Flow Metab.*, vol. 40, no. 5, pp. 922-938, 2020. Doi: 10.1177/0271678X20908363.

[4] H. Y. Um, B. H. Park, D. H. Ahn, M. I. Abd El Aal, J. Park, and H. S. Kim, "Mechanical and biological behavior of ultrafine-grained Ti alloy aneurysm clip processed using high-pressure torsion," *J. Mech. Behav. Biomed. Mater.*, vol. 68, no. September 2016, pp. 203-209, 2017. Doi: 10.1016/j.jmbbm.2017.02.002.

[5] F. Jumah, T. Quinoa, O. Akel, V. Narayan, N. Adeeb, G. Gupta, and A. Nanda, "The origins of eponymous aneurysm clips: A review," *World Neurosurg.*, vol. 134, pp. 518-531, 2020. Doi: 10.1016/j.wneu.2019.09.061.

[6] S. Liu and Y. C. Shin, "Additive manufacturing of Ti6Al4V alloy: A review," *Mater. Des.*, vol. 164, p. 107552, 2019. Doi: 10.1016/j.matdes.2018.107552.

[7] L.-C. Zhang and H. Attar, "Selective laser melting of titanium alloys and titanium matrix composites for biomedical applications: A review," *Adv. Eng. Mater.*, vol. 18, no. 4, pp. 463-475, 2016. Doi:

10.1002/adem.201500419.
[8] M. Geetha, A. K. Singh, R. Asokamani, and A. K. Gogia, "Ti based biomaterials, the ultimate choice for orthopaedic implants – A review," *Prog. Mater. Sci.*, vol. 54, no. 3, pp. 397-425, 2009. Doi: 10.1016/j.pmatsci.2008.06.004.
[9] A. Brack, S. Senger, G. Fischer, H. Janssen, J. Oertel, and C. Brecher, "Development of an artifact-free aneurysm clip," *Curr. Dir. Biomed. Eng.*, vol. 2, no. 1, 2016. Doi: 10.1515/cdbme-2016-0120.
[10] H. Demirturk Kocasarac, G. Ustaoglu, S. Bayrak, R. Katkar, H. Geha, S. Thomas Feahl, B. L Mealy, M. Danaci, and M. Noujeim, "Evaluation of artifacts generated by titanium, zirconium, and titanium–zirconium alloy dental implants on MRI, CT, and CBCT images: A phantom study," *Oral Surg. Oral Med. Oral Pathol. Oral Radiol.*, vol. 127, no. 6, pp. 535-544, 2019. Doi: 10.1016/j.oooo.2019.01.074.
[11] K. Ito, T. Seguchi, T. Nakamura, A. Chiba, T. Hasegawa, A. Nagm, T. Horiuchi, K. Hongo, "Evaluation of metallic artifacts caused by nonpenetrating titanium clips in postoperative neuroimaging," *World Neurosurg.*, vol. 96, pp. 16-22, 2016. Doi: 10.1016/j.wneu.2016.08.086.
[12] F. Khursheed, F. Rohlffs, S. Suzuki, D. H. Kim, and T. M. Ellmore, "Artifact quantification and tractography from 3T MRI after placement of aneurysm clips in subarachnoid hemorrhage patients," *BMC Med. Imaging*, vol. 11, no. 1, p. 19, 2011. Doi: 10.1186/1471-2342-11-19.
[13] L. Sonnow, S. Könneker, P. M. Vogt, F. Wacker, and C. Valcs, "Biodegradable magnesium Herbert screw – image quality and artifacts with radiography, CT and MRI," *BMC Medical Imaging*., pp. 17:16, 2017. Doi: 10.1186/s12880-017-0187-7.
[14] L. Sonnow, A. Ziegler, G. H. Pöhler, M. H. Kirschner, M. Richter, M. Cetin, M. Unal, and O. Kose, "Alterations in magnetic resonance imaging characteristics of bioabsorbable magnesium screws over time in humans: a retrospective single center study," *Innov Surg Sci*., pp. 105-113, 2017. Doi: 10.1515/iss-2021-0032.
[15] T. Wang, S. Inubushi, N. Ikeo, T. Mukai, K. Okumura, H. Akasaka, R. Yada, K. Yoshida, D. Miyawaki, T. Ishihara, A. Nakaoka, and R. Sasaki, "Novel artifact-robust and highly visible zinc solid fiducial marker for kilovoltage x-ray image-guided radiation therapy," *Med Phys*., vol 47, no 10, pp 4703-4710, 2020. Doi:10.1002/mp.14412.
[16] A. K. Mishra, P. Chalise, R. P. Singh, and R. K. Shah, "The proximal femur--a second look at rational of implant design," *Nepal Med. Coll. J.*, vol. 11, no. 4, pp. 278-280, 2009.
[17] W. S. Cho, K. I. Cho, J. E. Kim, T. S. Jang, E. J. Ha, H. S. Kang, Y. J. Son, S. H. Choi, S. Lee, C. C. Kim, J. Y. Sun, and H. E. Kim, "Zirconia-Polyurethane Aneurysm Clip," *World Neurosurg.*, vol. 115, pp. 14-23, 2018. Doi: 10.1016/j.wneu.2018.03.130.
[18] J. Kucinska-Lipka, I. Gubanska, and M. Sienkiewicz, "Thermal and mechanical properties of polyurethanes modified with L-ascorbic acid," *J. Therm. Anal. Calorim.*, vol. 127, no. 2, pp. 1631-1638, 2017. Doi: 10.1007/s10973-016-5743-9.
[19] A. N. Roziafanto, M. S. Dwijaya, R. Yunita, M. Amrullah, and M. Chalid, "Synthesis hybrid bio-polyurethane foam from biomass material," *Proceedings of the 5th International Symposium on Applied Chemistry 2019, AIP Conference Proceedings 2175*, p. 020068, 2019. Doi: 10.1063/1.5134632.
[20] J. Bandekar and S. Klima, "FT-IR spectroscopic studies of polyurethanes Part I. Bonding between urethane C-O-C groups and the NH Groups," *J. Mol. Struct.*, vol. 263, pp. 45–57, 1991, Doi: 10.1016/0022-2860(91)80054-8.
[21] S. A. Adnan, N. H. A. Zaidi, Y. M. Daud, and F. Zainuddin, "The effect of magnesium content on the properties of palm oil based polyurethane foam," *AIP Conference Proceedings 2030*, p. 020050, 2018. Doi: 10.1063/1.5066691.
[22] S. Yi, Y-J. Cho, and J-S. Roh, "Improved dimensional stability of water-blownpolyurethane foam with aluminum hydroxide and magnesium hydroxide," *J Appl Polym Sci.*, vol 137, no 46, p. 49510, 2020. Doi: 10.1002/app.49510.
[23] S. El Mogy, "Processing of polyurethane nanocomposite reinforced with nanosized zinc oxide: Effect on mechanical and acoustic properties," *Egypt. J. Chem.*, vol 62, no. 2, pp 333-341, 2018. Doi: 10.21608/ejchem.2018.4655.1410.
[24] J. Tomaszewska, T. Sterzyński, A. Woźniak-Braszak, and M. Banaszak,

"Review of recent developments of glass transition in PVC nanocomposites," *Polymers (Basel).*, vol. 13, no. 24, p. 4336, 2021. Doi: 10.3390/polym13244336.

[25] D. Filip, D. Macocinschi, and S. Vlad, "Thermogravimetric study for polyurethane materials for biomedical applications," *Compos. Part B Eng.*, vol. 42, no. 6, pp. 1474-1479, 2011. Doi: 10.1016/j.compositesb.2011.04.050.